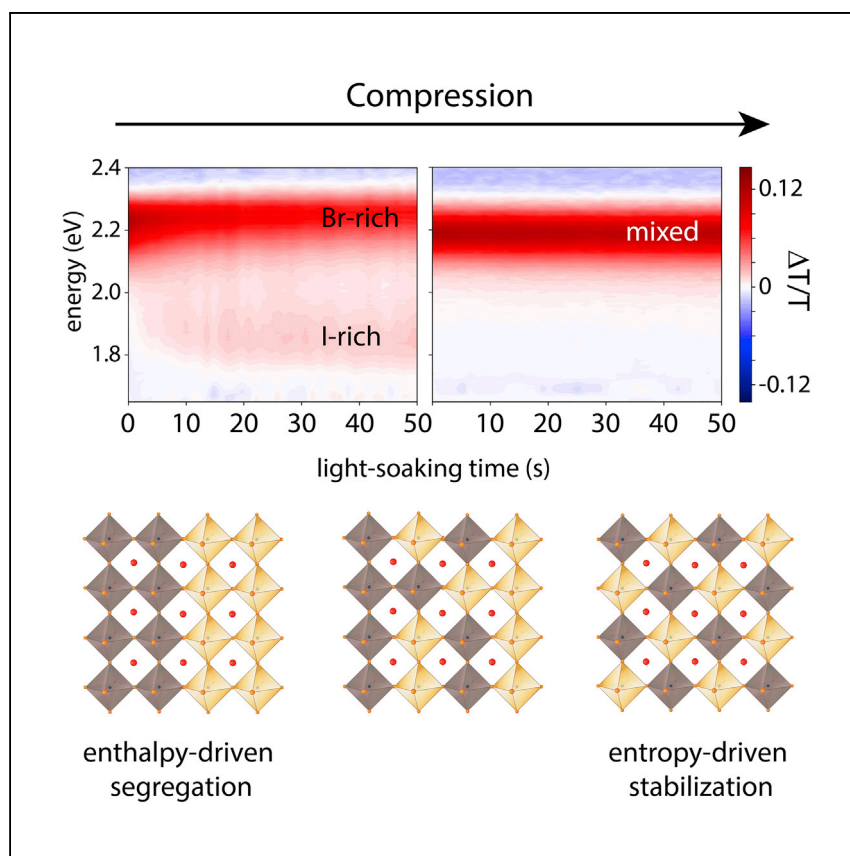## Report

Thermodynamic Stabilization of Mixed-Halide Perovskites against Phase Segregation

Eline M. Hutter, Loreta A. Muscarella, Francesca Wittmann, ..., Young-Kwang Jung, Aron Walsh, Bruno Ehrler

e.m.hutter@uu.nl (E.M.H.)
b.ehrler@amolf.nl (B.E.)

HIGHLIGHTS

Chemical and physical compression suppress segregation in mixed-halide perovskites

Pressure-dependent transient absorption is used to probe phase segregation in time

The halide mixing ratio in the segregated phase correlates with the unit cell volume

These findings are interpreted considering the $P\Delta V$ term of the Gibbs free energy

Mixed-halide perovskites could be the next-generation solar cell and LED material, but their composition and hence color of absorption and emission are unstable. Hutter et al. find that the range of thermodynamically stable compositions is substantially enlarged upon compression, guiding a more rational design toward color-tunable perovskites with stable emission.

Cell Reports
Physical Science

CellPress
OPEN ACCESS

Report

Thermodynamic Stabilization of Mixed-Halide Perovskites against Phase Segregation

Eline M. Hutter,[1,4,5,*] Loreta A. Muscarella,[1] Francesca Wittmann,[1] Jan Versluis,[1] Lucie McGovern,[1] Huib J. Bakker,[1] Young-Won Woo,[2] Young-Kwang Jung,[2] Aron Walsh,[2,3] and Bruno Ehrler[1,*]

SUMMARY

Mixing iodide and bromide in halide perovskite semiconductors is an effective strategy to tune their band gap; therefore, mixed-halide perovskites hold great promise for color-tunable LEDs and tandem solar cells. However, the band gap of mixed-halide perovskites is unstable under (sun-)light, since the halides segregate into domains of different band gaps. Using pressure-dependent ultrafast transient absorption spectroscopy, we find that high external pressure increases the range of stable halide mixing ratios. Chemical compression, by inserting a smaller cation, has the same effect, which means that any iodide:bromide ratio can be stabilized by tuning the crystal volume and compressibility. We interpret these findings as an increased thermodynamic stabilization through alteration of the Gibbs free energy via the largely overlooked $P\Delta V$ term.

INTRODUCTION

Metal halide perovskite semiconductors have recently received tremendous attention in materials science, as these have yielded highly efficient solar cells, light-emitting diodes (LEDs), and radiation detectors.[1-3] The unprecedented performance of perovskites is due to their outstanding optoelectronic properties, such as high optical absorption coefficients and relatively low trap densities, resulting in excellent charge transport and efficient radiative recombination.[4,5] Another key characteristic of metal halide perovskites is that their band gap is highly dependent on their chemical composition, meaning that any desired absorption onset or emission energy in the visible range can be obtained by tuning the composition. For instance, mixing iodide and bromide in $MAPb(I_{1-x}Br_x)_3$ (with methylammonium [MA], $CH_3NH_3^+$) results in band gaps intermediate to full iodide ($x = 0$, 1.6 eV) and full bromide ($x = 1$, 2.3 eV).[6,7] The combination of excellent optoelectronic properties and band gap tunability makes perovskites the most promising candidate for color-tunable LEDs as well as tandem solar cells,[8] in which multiple semiconductors with different band gaps are used to achieve optimum power conversion efficiencies.[9]

A major drawback of mixed-halide perovskites is that their band gap is unstable under illumination, since the halides segregate into iodide-rich and bromide-rich domains.[10,11] The lower-band gap iodide-rich domains act as charge carrier recombination centers, and this halide segregation is thus detrimental for device performance. It is essential, then, that the halide segregation is fully suppressed for any application of mixed-halide perovskites for which stable band gaps are required.

[1]AMOLF, Science Park 104, 1098 XG Amsterdam, the Netherlands

[2]Department of Materials Science and Engineering, Yonsei University, Seoul 03722, Korea

[3]Department of Materials, Imperial College London, London SW7 2AZ, UK

[4]Present address: Department of Chemistry, Utrecht University, Princetonlaan 8, 3584 CB Utrecht, the Netherlands

[5]Lead Contact

*Correspondence: e.m.hutter@uu.nl (E.M.H.), b.ehrler@amolf.nl (B.E.)

Previous studies have shown that halide segregation can be retarded by reducing the defect density and/or the illumination intensity.[12] However, achieving a commercially relevant stability on the timescale of 20 years may not be feasible through retardation alone (kinetic stability), as this would require a five orders of magnitude reduction in the segregation rate.[13] Unraveling design rules for thermodynamically stable mixed-halide perovskites will therefore be vital for band-gap-tunable perovskites with long-term stability. Under ambient conditions, the segregation of $MAPb(I_{1-x}Br_x)_3$ terminates at $x = 0.2$,[10,12] and segregation is absent if $x < 0.2$, which was attributed to a thermodynamic minimum in the Gibbs free energy.[14–16] In this work, we show that both external pressure and chemical compression shift this terminal x value (up to ~ 0.6), and, consequently, the range of thermodynamically stable mixing ratios is significantly extended under compression.[17] We extracted these terminal x values from transient absorption spectroscopy (TAS) measurements performed at hydrostatic pressures ranging from ambient to 0.3 GPa and for several initial mixing ratios x. In contrast to previously reported photoluminescence measurements at high pressure,[11] TAS allows us to track the formation of both the iodide- and bromide-rich domains during segregation. Hence, we find that at high pressure, both the iodide- and bromide-rich phases are closer to the initial x, and the terminal x value depends on both the external pressure and the initial composition. These findings can be understood from a change in the thermodynamics (Gibbs free energy) due to changes in the compressibility and the unit cell volume, providing an effective approach to obtain mixed-halide perovskites that are stable against photo-induced halide segregation. Consistently, we find that the chemical compression of the perovskite, via replacing MA ions with the smaller Cs ions, effectively suppresses halide segregation at ambient pressure. Our results show that stable mixed-halide perovskites of any desired halide composition can be designed by modifying the mechanical properties of the crystal so that the desired halide ratio falls in a miscible regime of the phase diagram, enabling a rational route toward thermodynamically stable mixed-halide perovskites.

RESULTS AND DISCUSSION

Thermodynamics of Phase Stability in Mixed-Halide Perovskites

The $MAPb(I_{1-x}Br_x)_3$ perovskite is an example of a pseudo-binary mixture (or solid solution). The accessible solubility range is determined by the free energy of mixing $\Delta G(x)$: the free energy of the mixed phase with respect to the phase-separated iodide ($x = 0$) and bromide ($x = 1$) compounds:

$$\Delta G(x) = \Delta H(x) - T\Delta S(x) \tag{Equation 1}$$

First-principles calculations of Equation 1 confirm a positive enthalpic term $\Delta H(x = 0.5) \sim 2$ kJ/mol due to chemical strain in the mixed $MAPb(I_{1-x}Br_x)_3$ perovskite,[14] which originates from the ionic size mismatch of I^- (2.22 Å) and Br^- (1.96 Å). The enthalpic cost of straining the bonding environment is offset by the gain in configurational entropy ($T\Delta S$).[14] For a binary mixture, the entropy reaches a maximum at $x = 0.5$, with a value also of ~ 2 kJ/mol (0.7 k_BT at $T = 300$ K). Analysis of $\Delta G(x)$ shows two minima (at $x \sim 0.2$ and at 0.75) under ambient conditions. The region in between these minima represents the miscibility gap (i.e., the range of compositions that are thermodynamically unstable). What has been overlooked thus far is that the enthalpy contains a $P\Delta V$ term in which pressure (P) can be used as an additional lever to control the stability range, which we explore in the following.

Reduced Segregation of Mixed-Halide Perovskites at High External Pressure

Thin films of mixed-halide $MAPb(I_{1-x}Br_x)_3$ with $0 < x < 1$ were spin coated from solution (see Experimental Procedures for procedures and Figure S1 for UV-VIS]
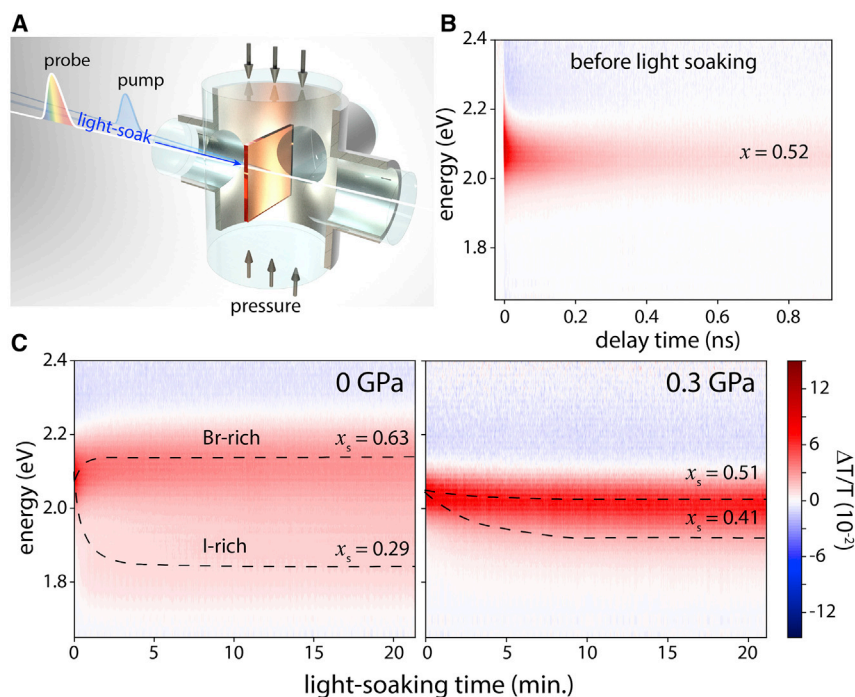
Figure 1. Pressure-Dependent Transient Absorption Spectroscopy of MAPb(I$_{1-x}$Br$_x$)$_3$ Thin Film before and after Light Soaking

(A) Schematic representation of the TAS setup, in which the MAPb(I$_{1-x}$Br$_x$)$_3$ thin film is placed inside a hydraulic pressure cell. The pressure can be increased by adding more liquid, and the pump, probe, and CW laser enter this cell via quartz windows.

(B) $\Delta T/T$ as a function of energy and delay time for $x = 0.52 \pm 0.04$ before light soaking.

(C) $\Delta T/T$ as a function of energy during 20 min of light soaking with the CW laser ($\lambda = 405$ nm, $I = 2.37 \times 10^3$ mW/cm^2) at 0 GPa (left) and 0.3 GPa (right). At ambient pressure (left), light soaking leads to segregation into iodide-rich ($x_s = 0.29 \pm 0.02$) and bromide-rich ($x_s = 0.63 \pm 0.05$) domains, while light soaking at 0.3 GPa leads only to the formation of a small side peak corresponding to $x_s = 0.41 \pm 0.03$.

and X-ray diffraction [XRD]), and their initial stoichiometries x were determined from scanning electron microscopy-energy-dispersive X-ray spectroscopy (SEM-EDX). The initial band gaps vary from 1.6 eV ($x = 0$) to 2.3 eV ($x = 1$). However, the band gaps of $0.2 < x < 1$ are unstable under illumination with a continuous wave (CW) laser, showing photoluminescence (PL) emission energies of 1.68–1.75 eV, independent of x (see Figure S2). This band gap instability has been widely observed in mixed-halide perovskites[10,18–20] and is attributed to segregation of the halides into iodide- and bromide-rich domains. After segregation, all light emission originates from the iodide-rich domains, which have a lower band gap. Therefore, this halide segregation is detrimental for perovskite-based LEDs if their desired emission energy falls in between 1.7 and 2.3 eV. Segregation is also unfavorable for perovskite-based solar cells, as the voltage is lowered by ΔE, the difference between the original band gap and the energy of the iodide-rich region.[19] The shared emission energy of ~1.7 eV corresponds to a segregated composition x_s ~0.2, and the MAPb(I$_{1-x}$Br$_x$)$_3$ perovskite is unstable if $x > x_s$ (= 0.2 under ambient conditions).[10,21] Since this threshold coincides with a cubic-to-tetragonal phase transition at approximately room temperature, it was previously proposed that this phase transition impedes full halide segregation.[20,21] As we show below, however, this assignment is inconsistent with the behavior of mixed-halide perovskites under hydrostatic pressure.

We used pressure-dependent TAS measurements, as shown in Figure 1A, to follow the segregation in time for different initial mixing ratios and pressures. While PL measurements only probe emissive phases, and thus often only probe the iodide-rich phase,[10,17] TAS measures the bleach from each excited state population and hence allows us to obtain a complete picture of the energetic landscape, tracing both the formation of iodide-rich and bromide-rich phases.[22,23] We aligned the pump and probe inside a hydraulic pressure cell and filled it with the perovskite thin film and an inert liquid (degassed perfluorohexane, see Experimental Methods). Increasing the liquid content in the cell increases the hydrostatic pressure up to 0.3 GPa. We note that this pressure range is low enough to avoid any phase transitions in the $MAPb(I_{1-x}Br_x)_3$ perovskites, as confirmed by pressure-dependent UV-VIS measurements (see Figure S3).

Figure 1B shows $\Delta T/T$ as a function of energy and delay time t_d (time after excitation) for a thin $MAPb(I_{1-x}Br_x)_3$ film, with $x = 0.52 \pm 0.04$. The positive (bleach) signal peaking at 2.02 eV corresponds to the ground state bleach (GSB) of the perfectly mixed iodide-bromide perovskite. The recombination of these charges then leads to a reduction in $\Delta T/T$ at increased t_d.

To investigate the effect of light soaking on the energetic landscape of the perovskite, we illuminated the sample with a CW (intensity equivalent to 24 suns) laser for 20 min. This relatively high light-soaking intensity was used so that we could perform the measurement within a reasonable time frame, especially at the higher pressures. A fixed delay time of ~15 ps was used, which is before recombination and energy transfer events but after cooling of the charges into the iodide- and bromide-rich domains.[23,24] As shown in Figure 1C, two positive features appear within several minutes of light soaking, indicating the segregation into iodide- and bromide-rich domains, with band gaps of 1.84 and 2.11 eV, respectively (see also Figure S4). These energies correspond to x_s values of 0.29 ± 0.02 for the iodide-rich phase and $x_s = 0.63 \pm 0.05$ for the bromide-rich phase (see Figure S5). In contrast, light soaking the same mixed-halide perovskite at high pressure (0.3 GPa) does not lead to the formation of distinct iodide and bromide phases. Instead, only a small side peak appears corresponding to $x_s = 0.41 \pm 0.03$, next to the initial $\Delta T/T$ peak ($x_s = 0.51 \pm 0.04$). This observation shows that halide segregation is substantially suppressed at high pressure.

Pressure Effects on the Halide Mixing Ratio in the Segregated Phases

Figures 2A–2C show $\Delta T/T$ during light soaking at ambient pressure for mixed-halide perovskites, with $x = 0.25$ (Figure 2A), $x = 0.5$ (Figure 2B), and $x = 0.7$ (Figure 2C). The initial GSBs peaking at 2.1 eV (at 15 ps) for $x = 0.5$ (Figure 2B) and 2.2 eV for $x = 0.7$ (Figure 2C) shift to higher energies during light soaking, while reducing in magnitude. Simultaneously, an ingrowth of a relatively broad peak is observed at ~1.9 eV, due to the formation of the iodide-rich phase. For $x = 0.25$, the GSB slightly red shifts 30 meV during light soaking, without the formation of a (detectable) second phase (see Figure 2A). Similarly, no phase segregation is observed on light soaking for $x = 0.1$ (see Figure S6), which is consistent with previously reported PL measurements showing stable band gaps for $x < 0.2$.[21]

While the iodide-rich phase has the same final composition independent of initial composition (at ambient pressure), we find that the bromide-rich phase changes substantially with x, as indicated by the different positions of the high-energy peaks in Figures 2B and 2C. This trend suggests that the iodide-rich domains form by the
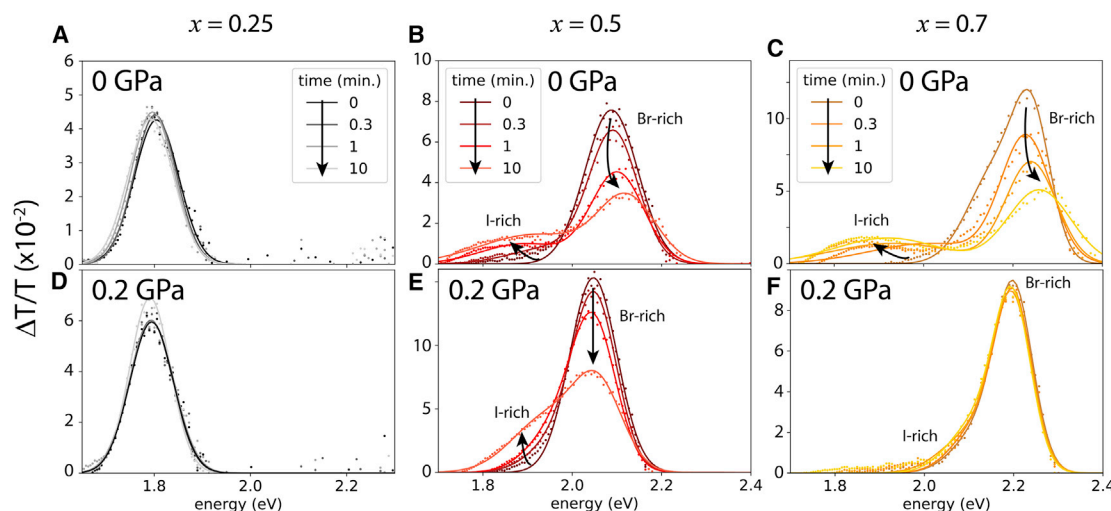
Cell Reports
Physical Science
Report

Figure 2. Band Gap Evolution during Light Soaking for Different Initial Compositions at Ambient versus High External Pressure

(A–F) Transient absorption spectra (recorded at 15 ps time delay) after 0, 0.3, 1, and 10 min of light soaking at ambient pressure using CW illumination (405 nm, 2.37×10^3 mW/cm^2) for initial composition $x = 0.25$ (A), $x = 0.5$, (B), and $x = 0.7$ (C) and at high pressure for initial composition $x = 0.25$ (D), $x = 0.5$ (E), and $x = 0.7$ (F).

Note that (B) and (E) correspond to the sample shown in Figure 1.

migration of iodide toward the initially formed centers, and that the bromide-rich domains form simply by the depletion of iodide from the mixed phase.

Figures 2D–2F show the $\Delta T/T$ during light soaking at a pressure of 0.2 GPa; other pressures are shown in Figures S7–S9. We find that for an initial composition of $x = 0.25$, the perovskite is entirely stable against phase segregation at 0.2 GPa. In addition, in sharp contrast to the ambient pressure results (Figures 2B and 2C), the segregated iodide-rich phases of perovskites with initial composition $x = 0.5$ and $x = 0.7$ no longer occur at the same energy at 0.2 GPa. That is, $x = 0.5$ (Figure 2D) shows a clear ingrowth of the iodide-rich phase at 1.89 eV, while the $x = 0.7$ remains mostly stable, showing only a small side peak at 2.0 eV. These energies correspond to $x_s = 0.37 \pm 0.03$ (for $x = 0.5$) and $x_s = 0.51 \pm 0.04$ (for $x = 0.7$), which means that at high pressure, the segregated iodide-rich phase has a different composition, depending on the initial composition (see Figure S10 for $\Delta T/T$ as a function of delay time). The observation that x_s does vary with x at high pressure (in contrast to the situation at ambient pressure; see also Table S1) is a first indication that x_s is not determined by the cubic-to-tetragonal phase transition. In addition, Jaffe et al.[11] reported that both $x = 0.2$ and $x = 0.4$ are still in the cubic phase at 0.5 GPa, which means that the phase transition does not shift to higher x values within this pressure range. Therefore, the cubic-to-tetragonal phase transition is not the reason for the observed shifts in the terminal x at high pressure.

The Unit Cell Volume as a Key Factor Determining Phase Stability of Mixed-Halide Perovskites

As an alternative explanation, we consider the mechanical effects associated with the less compressible and smaller unit cell volume for samples with higher bromide content as the origin of the reduced segregation. Since MAPbBr$_3$ has a larger bulk modulus than MAPbI$_3$,[11,25] the volume change upon applying pressure to the mixed-halide MAPb(I$_{1-x}$Br$_x$)$_3$ perovskite is smaller for higher bromide contents (see Figure S11). Figure 3A shows x_s of the iodide-rich phase (squares) and bromide-rich phase (open circles) as a function of the unit cell volume, obtained from
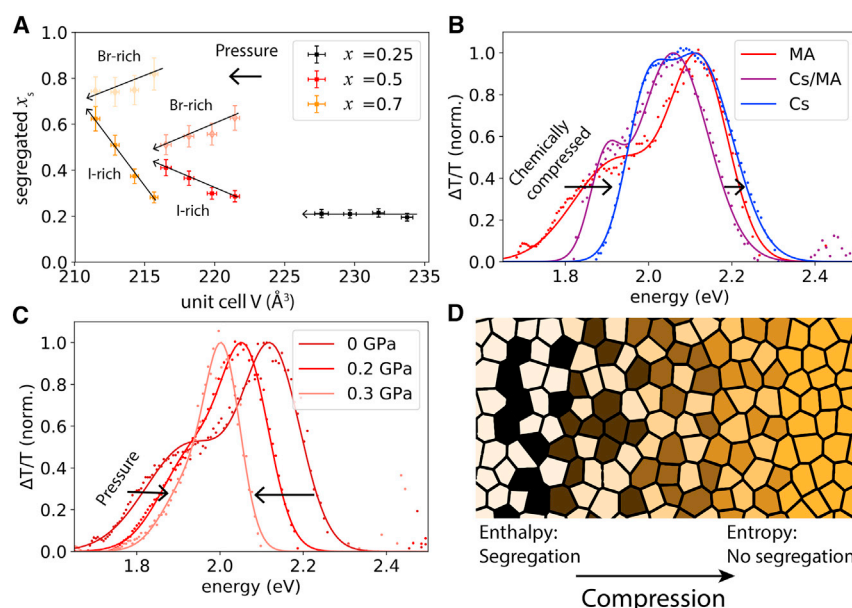
Figure 3. Comparison between Physical and Chemical Compression as a Route toward Enlarging the Stability Window of Mixed-Halide Perovskites

(A) Composition (x_s) of low-band gap (I-rich) and high-band gap (Br-rich) phases in MAPb($I_{1-x}Br_x$)$_3$ after segregation, plotted against initial (average) unit cell volume. The error bars on the unit cell volume were calculated from the error in the pressure-dependent bulk modulus (Figure S11), and the error on x_s from the band gap versus x (fits in Figure S5). Arrows are included to guide the eye.

(B and C) Normalized transient absorption spectra (t_d = 15 ps) after 20 min of light soaking a chemically (B) and a physically (C) compressed x = 0.5 mixed-halide perovskite. The samples shown in (B) correspond to MAPbI$_{1.5}$Br$_{1.5}$ (red), MA$_{0.5}$Cs$_{0.5}$PbI$_{1.5}$Br$_{1.5}$ (purple), and CsPbI$_{1.5}$Br$_{1.5}$ (blue).

(D) Schematic representation of the suppression of segregation by compressing the mixed-halide perovskite. The orange color (on the right side of the panel) represents the initial mixing ratio, and the light- and dark-colored regions represent Br- and I-rich grains, respectively. At ambient pressure, the positive mixing enthalpy for MAPb($I_{1-x}Br_x$)$_3$ drives photo-induced segregation at x > 0.2.[14,15] For higher pressure or Cs content, with smaller unit cell volumes, the mixing enthalpy is reduced so that the entropy dominates for a larger range of mixing ratios. As a result, the segregated mixing ratios are closer to the initial mixing ratio (in orange) in compressed perovskites.

pressure-dependent TAS measurements of segregated samples with initial stoichiometries of of x = 0.25 (black), 0.5 (red), and 0.7 (yellow). Note that the largest volume for each x corresponds to ambient pressure, and the smallest volume corresponds to 0.3 GPa. We find that the stable iodide-rich composition significantly shifts with changes in the unit cell volume V, increasing from the previously observed $x \sim 0.2$ (for V > 218 Å^3) to $x \sim 0.6$ (for V = 209 Å^3; x = 0.7 at 0.3 GPa).

These observations show that the unit cell volume is an important factor determining the x values at which mixed-halide perovskites are stable. We found that chemically compressing x = 0.5 by replacing 50% of MA with smaller Cs cations reduces the halide segregation roughly to the same extent as applying 0.2 GPa external pressure to the pure MA cation perovskite (see Figures 3B and 3C). Note that Cs-based perovskites have larger band gaps than MA-based perovskites,[26] so that the absolute peak energies cannot be compared between Figures 3B and 3C. On fully exchanging the MA with Cs for x = 0.5, the band gap is almost completely stabilized against segregation, and the energy difference between the 2 peaks is only $\sim$100 meV, similar to applying 0.3 GPa to the MA perovskite (see Figure 3C). Whereas the pressure-dependent measurements on MAPb($I_{1-x}Br_x$)$_3$ allowed us to isolate the

effect of pressure, reducing the unit cell by mixing in Cs may lead to changes in the defect density or the halide ratio. Therefore, a one-to-one relation between the physical and chemical pressures cannot be made. However, the observation that stability can be improved upon decreasing the unit cell volume, either physically or chemically, suggests that compressing the unit cell is a general route toward the improved stability observed in Cs-based perovskites.[18,27]

We rationalize these observations from an alteration of x_s due to the $P\Delta V$ term in the free energy of mixing (Equation 1). Whereas ΔS is unchanged under the mild pressure we apply, due to a regular perovskite structure being maintained, the previously neglected $P\Delta V$ term does change $\Delta H(x)$. As the bulk modulus of the iodide (9 GPa for $MAPbI_3$) is much smaller than the bromide (18 GPa for $MAPbBr_3$), the iodide-rich regions undergo a larger volume change and pay a larger enthalpic penalty. From continuum mechanics, the combination of $P = 0.3$ GPa and $x = 0.5$ results in $\Delta V = 5$ Å^3, and $P\Delta V = 1$ kJ/mol. Given that the magnitude of $T\Delta S$ is limited to 2 kJ/mol, this represents a substantial contribution. In addition, the higher compressibility of iodide means that the ionic size mismatch decreases with pressure, which will lower the microscopic strain of the mixed system and allow $T\Delta S$ to dominate and stabilize the mixture for larger values of x (see Figure 3D). We note that the magnitude of the terms involved here are small and are likely to result in an ensemble of ion configurations and distributions accessible around room temperature.

The observation that segregation only occurs under light requires a modification of the equilibrium thermodynamics (Equation 1)[14] in the presence of electronic excitations.[15] Local inhomogeneities in halide distribution may result in low-band gap regions (already present in the dark),[28] which act as traps to photoexcited holes. The band gap difference ΔE_g between the high- and low-band gap domains then provides the driving force for the light-induced phase segregation process.[15] This electronic term in the phase diagram is expected not to change significantly with pressure, as the band gaps of both the iodide and bromide compounds and their mixtures show a similar pressure dependence (see also Figure S12). However, the pressure-induced shift in minimum ΔG (dark) significantly extends the miscible regime of x in compressed perovskites and thus, the range of compositions that is entropically stabilized.

Previous approaches to suppress halide segregation are mainly based on the reduction in iodide vacancies, for instance, by adding potassium iodide or using an excess of halides during the synthesis.[23,29] The reduction in vacancies lowers the density of mobile ions, which considerably slows ion migration and consequently the halide segregation. Slowing down the rate of halide segregation is an effective approach to kinetically stabilize mixed-halide perovskites.[15] However, as long as these systems are thermodynamically unstable, they are still prone to segregate slowly and hence, thermodynamic stabilization achieved through manipulating the unit cell is the only route to applications of mixed-halide perovskites that require long-term (i.e., many decades) stability.

In conclusion, we have shown that compressing mixed-halide $MAPb(I_{1-x}Br_x)_3$ perovskite thin films, either via applying external pressure or via reducing the cation size, greatly improves their stability against photoinduced halide segregation. Using pressure-dependent TAS, we followed the compositional changes in both the iodide- and the bromide-rich phases associated with segregation. Whereas at ambient pressure, the segregation discontinues if the iodide-rich phase reaches $x_s \sim 0.2$, this threshold is substantially shifted with pressure, reaching $x_s \sim 0.6$ at 0.3 GPa for an initial mixing ratio of $x = 0.7$. We interpret these findings from an alteration of the Gibbs free energy via the $P\Delta V$ term, which was initially overlooked in the theoretical calculations. This term, which is larger than traditional inorganic semiconductors allows, owing to the mechanical

CellPress
OPEN ACCESS

Cell Reports
Physical Science
Report

softness of halide perovskites, provides a lever to extend the range of thermodynamically stable mixed-halide compositions by increasing the pressure or decreasing the volume. These results suggest that any iodide:bromide ratio could in principle be thermodynamically stabilized against halide segregation by tuning the crystal volume and compressibility, enabling full band gap tunability of stable mixed-halide perovskites.

EXPERIMENTAL PROCEDURES

Resource Availability

Lead Contact
Dr. Eline Hutter: e.m.hutter@uu.nl.

Materials Availability
The samples used in this study have degraded and are no longer available.

Data and Code Availability
All data are included in the paper and the Supplemental Information. Raw data files are available on request.

Sample Fabrication
Quartz substrates were sonicated with deionized water, acetone, and isopropanol sequentially for 15 min, followed by an oxygen plasma treatment for 20 min at 100 W. The solvents N,N-dimethylformamide (DMF; Sigma-Aldrich anhydrous, $\geq$99%) and dimethylsulfoxide (DMSO; Sigma-Aldrich anhydrous, $\geq$99.9%) were mixed in a 4:1 (DMF:DMSO) volume ratio. The solvent mixtures were used to prepare stock solutions of lead iodide (TCI; 99.99%, trace metals basis), CH_3NH_3I (MAI; TCI, >99%), lead bromide (Sigma-Aldrich, trace metals basis), and CH_3NH_3Br (MABr; TCI, >98%) by dissolving these precursors at 1.1 M. $MAPbI_3$ and $MAPbBr_3$ solutions were prepared by mixing the MAI with PbI_2 and MABr with $PbBr_2$ stock solutions at 1:1 molar stoichiometric ratios (i.e., 1:1 v:v). Stock solutions of $CsPbI_3$ and $CsPbBr_3$ were prepared by dissolving 1:1 molar stoichiometric ratios of CsI (Sigma, 99.999%) with lead iodide and CsBr (TCI, >98%) with lead bromide in dimethyl sulfoxide (DMSO, Sigma Aldrich anhydrous, $\geq$99%) to obtain 0.4 M as final concentration, respectively. The $MAPb(I_{1-x}Br_x)_3$ precursor solutions were prepared by mixing x parts $MAPbBr_3$ stock solution with $(1 - x)$ parts $MAPbI_3$ stock solution, resulting in 1.1 M $MAPb(I_{1-x}Br_x)_3$ solutions. For the mixed-cation mixed-halide perovskites, $MAPb(I_{1-x}Br_x)_3$ and $CsPb(I_{1-x}Br_x)_3$ solutions were first prepared according to the desired halide mixing ratio, both at 0.4 M, and then mixed according to the desired cation ratio. The films were prepared by spin coating the precursor solutions on quartz substrates at 9,000 rpm for 30 s and the anti-solvent of chlorobenzene (Sigma-Aldrich, anhydrous, $\geq$99%) was dropped 15 s after the start of spin coating, followed by thermal annealing at 100°C for 1 h. Both the preparation and spin coating of solutions were done in a nitrogen-filled glovebox.

Characterization
The XRD patterns of the perovskite films deposited on quartz were measured using an X-ray diffractometer, Bruker D2 Phaser, with Cu Kα (λ = 1.541 Å) as the X-ray source, 0.05° (2θ) as the step size, and 0.150 s as the exposure time. Elemental analysis (EDX) was performed using an FEI Verios 460 field emission scanning electron microscope operated at 7 kV. Pressure-dependent transmission spectra of the $MAPb(I_{1-x}Br_x)_3$ films were measured from 850 nm to 350 nm using a pressure cell (ISS) and a LAMBDA 750 UV/Vis/NIR (near-infrared) spectrophotometer (Perkin-Elmer). The absorption at ambient pressure was determined by measuring the transmission and reflection inside the integrating sphere.

TAS under Hydrostatic Pressure

During the measurement, the sample was kept inside a high-pressure cell (ISS) filled with the inert pressurizing liquid Fluorinert FC-72 (3M). Before use, the liquid was degassed in a Schlenk line by bubbling N to remove O and water. The hydrostatic pressure was generated by increasing the amount of the pressurizing liquid in the cell using a manual pump. The pressure was increased from ambient to 0.3 GPa in steps of 0.1 GPa, with an error of 0.02 GPa estimated from reading the pressure on the gauge (unless at ambient pressure). At every pressure, we waited 7 min for equilibration of the material under pressure. TA spectra were collected using a homemade setup operating in a non-degenerate pump-probe configuration. The laser source for the TA is a regenerative Ti:sapphire amplifier (Coherent) producing a fundamental beam characterized by 800-nm pulses at a 1-kHz repetition rate, with a pulse duration of 35 fs and a pulse energy of 6.5 mJ. The fundamental beam is split into two beams by a beam splitter. After chopping the beam in the pump path (using 500 Hz as the frequency), a 400-nm pulse pump was generated by doubling an 800-nm pulse with a beta barium borate (BBO) crystal. A short-pass filter was placed after the BBO crystal in the pump path to remove 800-nm residue from the fundamental beam. The white light continuum probe pulses were produced by focusing the 800-nm femtosecond pulses through a 2-mm sapphire plate. The probe spot size was chosen to be smaller than the pump spot size to obtain homogeneous excitation over the probed area. The two beams were then spatially overlapped inside the pressure cell. To follow the evolution in time of the system, the pump-probe delay time was changed from 0 to 1,000 ps using a mechanical delay stage. Unless stated otherwise, the pump excitation density was $\sim10^{18}$ cm^{-3} (see Figure S13 for different excitation densities). The samples were light soaked using a 405-nm CW single-mode fiber-coupled laser source (Thorlabs). The CW laser was focused on the same spot as the pump and probe, and its spot size (243 μm diameter) was large enough to fully cover the probed area (<50 μm). The intensity of the light-soaking source was 2.37×10^{3} mW/cm^{2} ($\sim$24 suns), and no segregation was observed in the absence of the CW source (see Figure S14).

SUPPLEMENTAL INFORMATION

Supplemental Information can be found online at https://doi.org/10.1016/j.xcrp.2020.100120.

AUTHOR CONTRIBUTIONS

E.M.H. conceived the idea and performed the pressure-dependent TA experiments and data analysis together with L.A.M., under the supervision of B.E. F.W. performed the XRD and pressure-dependent UV-VIS measurements and assisted in the sample preparation together with L.M. J.V. assisted in the TA experiments under the supervision of H.J.B. Thermodynamic calculations were performed by A.W., Y.-W.W., and Y.-K.J. The manuscript was written by E.M.H. and A.W., with input from all of the other authors.

CellPress
OPEN ACCESS

Cell Reports
Physical Science
Report

DECLARATION OF INTERESTS

The authors declare no competing interests.

REFERENCES

1. Kojima, A., Teshima, K., Shirai, Y., and Miyasaka, T. (2009). Organometal halide perovskites as visible-light sensitizers for photovoltaic cells. J. Am. Chem. Soc. 131, 6050–6051.

2. Yakunin, S., Sytnyk, M., Kriegner, D., Shrestha, S., Richter, M., Matt, G.J., Azimi, H., Brabec, C.J., Stangl, J., Kovalenko, M.V., and Heiss, W. (2015). Detection of X-ray photons by solution-processed organic-inorganic perovskites. Nat. Photonics 9, 444–449.

3. Song, J., Li, J., Li, X., Xu, L., Dong, Y., and Zeng, H. (2015). Quantum Dot Light-Emitting Diodes Based on Inorganic Perovskite Cesium Lead Halides (CsPbX3). Adv. Mater. 27, 7162–7167.

4. Brenner, T.M., Egger, D.A., Kronik, L., Hodes, G., and Cahen, D. (2016). Hybrid organic-inorganic perovskites: low-cost semiconductors with intriguing charge-transport properties. Nat. Rev. Mater. 1, 15007.

5. Manser, J.S., Christians, J.A., and Kamat, P.V. (2016). Intriguing Optoelectronic Properties of Metal Halide Perovskites. Chem. Rev. 116, 12956–13008.

6. Jeon, N.J., Noh, J.H., Yang, W.S., Kim, Y.C., Ryu, S., Seo, J., and Seok, S.I. (2015). Compositional engineering of perovskite materials for high-performance solar cells. Nature 517, 476–480.

7. Noh, J.H., Im, S.H., Heo, J.H., Mandal, T.N., and Seok, S.I. (2013). Chemical management for colorful, efficient, and stable inorganic-organic hybrid nanostructured solar cells. Nano Lett. 13, 1764–1769.

8. McMeekin, D.P., Sadoughi, G., Rehman, W., Eperon, G.E., Saliba, M., Hörantner, M.T., Haghighirad, A., Sakai, N., Korte, L., Rech, B., et al. (2016). A mixed-cation lead mixed-halide perovskite absorber for tandem solar cells. Science 351, 151–155.

9. De Vos, A. (1980). Detailed balance limit of the efficiency of tandem solar cells. J. Phys. D Appl. Phys. 13, 839–846.

10. Hoke, E.T., Slotcavage, D.J., Dohner, E.R., Bowring, A.R., Karunadasa, H.I., and McGehee, M.D. (2015). Reversible photo-induced trap formation in mixed-halide hybrid perovskites for photovoltaics. Chem. Sci. 6, 613–617.

11. Jaffe, A., Lin, Y., Beavers, C.M., Voss, J., Mao, W.L., and Karunadasa, H.I. (2016). High-pressure single-crystal structures of 3D lead-halide hybrid perovskites and pressure effects on their electronic and optical properties. ACS Cent. Sci. 2, 201–209.

12. Brennan, M.C., Ruth, A., Kamat, P.V., and Kuno, M. (2020). Photoinduced Anion Segregation in Mixed Halide Perovskites. Trends Chem. 2, 282–301.

13. Ehrler, B., and Hutter, E.M. (2020). Routes toward Long-Term Stability of Mixed-Halide Perovskites. Matter 2, 800–802.

14. Brivio, F., Caetano, C., and Walsh, A. (2016). Thermodynamic Origin of Photoinstability in the CH3NH3Pb(I1-xBrx)3 Hybrid Halide Perovskite Alloy. J. Phys. Chem. Lett. 7, 1083–1087.

15. Draguta, S., Sharia, O., Yoon, S.J., Brennan, M.C., Morozov, Y.V., Manser, J.S., Kamat, P.V., Schneider, W.F., and Kuno, M. (2017). Rationalizing the light-induced phase separation of mixed halide organic-inorganic perovskites. Nat. Commun. 8, 200.

16. Wang, X., Ling, Y., Lian, X., Xin, Y., Dhungana, K.B., Perez-Orive, F., Knox, J., Chen, Z., Zhou, Y., Beery, D., et al. (2019). Suppressed phase separation of mixed-halide perovskites confined in endotaxial matrices. Nat. Commun. 10, 695.

17. Jaffe, A., Lin, Y., and Karunadasa, H.I. (2017). Halide Perovskites under Pressure: Accessing New Properties through Lattice Compression. ACS Energy Lett. 2, 1549–1555.

18. Beal, R.E., Slotcavage, D.J., Leijtens, T., Bowring, A.R., Belisle, R.A., Nguyen, W.H., Burkhard, G.F., Hoke, E.T., and McGehee, M.D. (2016). Cesium lead halide perovskites with improved stability for tandem solar cells. J. Phys. Chem. Lett. 7, 746–751.

19. Samu, G.F., Janáky, C., and Kamat, P.V. (2017). A Victim of Halide Ion Segregation. How Light Soaking Affects Solar Cell Performance of Mixed Halide Lead Perovskites. ACS Energy Lett. 2, 1860–1861.

20. Brennan, M.C., Draguta, S., Kamat, P.V., and Kuno, M. (2018). Light-Induced Anion Phase Segregation in Mixed Halide Perovskites. ACS Energy Lett. 3, 204–213.

21. Unger, E.L., Kegelmann, L., Suchan, K., Sörell, D., Korte, L., and Albrecht, S. (2017). Roadmap and roadblocks for the band gap tunability of metal halide perovskites. J. Mater. Chem. A 5, 11401–11409.

22. Yoon, S.J., Kuno, M., and Kamat, P.V. (2017). Shift Happens. How Halide Ion Defects Influence Photoinduced Segregation in Mixed Halide Perovskites. ACS Energy Lett. 2, 1507–1514.

23. Barker, A.J., Sadhanala, A., Deschler, F., Gandini, M., Senanayak, S.P., Pearce, P.M., Mosconi, E., Pearson, A.J., Wu, Y., Srimath Kandada, A.R., et al. (2017). Defect-Assisted Photoinduced Halide Segregation in Mixed-Halide Perovskite Thin Films. ACS Energy Lett. 2, 1416–1424.

24. Price, M.B., Butkus, J., Jellicoe, T.C., Sadhanala, A., Briane, A., Halpert, J.E., Broch, K., Hodgkiss, J.M., Friend, R.H., and Deschler, F. (2015). Hot-carrier cooling and photoinduced refractive index changes in organic-inorganic lead halide perovskites. Nat. Commun. 6, 8420.

25. Sun, S., Fang, Y., Kieslich, G., White, T.J., and Cheetham, A.K. (2015). Mechanical properties of organic-inorganic halide perovskites, CH3NH3PbX3 (X = I, Br and Cl), by nanoindentation. J. Mater. Chem. A 3, 18450–18455.

26. Eperon, G.E., Paterno, G.M., Sutton, R.J., Zampetti, A., Haghighirad, A.A., Cacialli, F., and Snaith, H.J. (2015). Inorganic caesium lead iodide perovskite solar cells. J. Mater. Chem. A 3, 19688–19695.

27. Beal, R.E., Zhou Hagström, N., Barrier, J., Gold-Parker, A., Prasanna, R., Bush, K.A., Passarello, D., Schelhas, L.T., Brüning, K., Tassone, C.J., et al. (2020). Structural origins of light-induced phase segregation in organic-inorganic halide perovskite photovoltaic materials. Matter 2, 1–13.

28. Feldmann, S., Macpherson, S., Senanayak, S.P., Abdi-jalebi, M., Rivett, J.P.H., Nan, G., Tainter, G.D., Doherty, T.A.S., Frohna, K., Ringe, E., et al. (2020). Photodoping through local charge carrier accumulation in alloyed hybrid perovskites for highly efficient luminescence. Nat. Photonics 14, 123–128.

29. Abdi-Jalebi, M., Andaji-Garmaroudi, Z., Cacovich, S., Stavrakas, C., Philippe, B., Richter, J.M., Alsari, M., Booker, E.P., Hutter, E.M., Pearson, A.J., et al. (2018). Maximizing and stabilizing luminescence from halide perovskites with potassium passivation. Nature 555, 497–501.